Multiple stages of plant root calcification deciphered by chemical and micromorphological analyses

Arnaud Huguet, Sylvain Bernard, Rime El Khatib, Martina I Gocke, Guido L.B. Wiesenberg, Sylvie Derenne

Multiple stages of plant root calcification deciphered by chemical and micromorphological analyses

Arnaud Huguet [a*], Sylvain Bernard [b], Rime El Khatib [a, b], Martina I. Gocke [c,d], Guido L.B. Wiesenberg [d], Sylvie Derenne [a]

[a] *Sorbonne Université, CNRS, EPHE, PSL, UMR METIS, F-75005 Paris, France*
[b] *MNHN, CNRS, Sorbonne Université, UMR IMPMC, F-75005, Paris, France*
[c] *University of Bonn, Institute of Crop Science and Resource Conservation, Division Soil Science, D-53115 Bonn, Germany*
[d] *Department of Geography, University of Zurich, Winterthurerstrasse 190, 8057 Zürich, Switzerland*

Acknowledgments

The authors thank Labex MATISSE (Sorbonne Universités) for funding of R. El Khatib's postdoctoral fellowship. The financial support of CNRS through the PICS program is also acknowledged. C. Anquetil is thanked for help with ^{13}C NMR analyses. Sample collection and preparation was performed as part of a DFG (German Research Foundation, project 184773399) and a SNF (Swiss National Science Foundation, project 153631) project.

Data availability statement

The data that support the findings of this study are available from the corresponding author upon reasonable request.

[*] Corresponding author. Tel: + 33-144-275-172; fax: +33-144-275-150.
E-mail address: arnaud.huguet@sorbonne-universite.fr (A. Huguet).

ABSTRACT

Rhizoliths, i.e. roots fossilized by secondary carbonates, have been known for ages and are increasingly used for paleoenvironmental reconstructions. However, knowledge about their formation mechanisms remains limited. This study reports the mineralogical and chemical characterization of rhizoliths at different stages of mineralization and fossilization in the Late Pleistocene loess-paleosol sequence of Nussloch (SW Germany). Scanning electron microscopy coupled with elemental mapping and ^{13}C solid-state nuclear magnetic resonance were used to concomitantly characterize the mineral and organic matter of the rhizoliths. These joint analyses showed for the first time that large rhizoliths are not necessarily remains of single large roots, but consist of numerous microrhizoliths as remains of fine roots, formed mainly by calcium carbonates with only low amounts of Mg and Si. They further revealed that the precipitation of secondary carbonates occurs not only around, but also within the plant root and that fossilization leads to the selective preservation of recalcitrant root biopolymers – lignin and suberin. The precipitation of secondary carbonates was observed to occur first around fine roots, the epidermis acting as a first barrier, and then within the root, within the cortex cells and even sometimes around the phloem and within the xylem. This study suggests that the calcification of plant roots starts during the lifetime of the plant and continues after its death. This has to be systematically investigated to understand the stratigraphic context before using (micro)rhizoliths for paleoenvironmental reconstructions in terrestrial sediments.

Keywords: rhizoliths; SEM; ^{13}C NMR; loess sediments; secondary carbonates; organic matter; paleoenvironment

1. Introduction

Rhizoliths have been ascribed different names, e.g. root casts; rhizocretions; tubular fossils (Klappa, 1980), and may exhibit different morphologies and sizes (up to several cm in diameter and several meters length; Zamanian et al., 2016). These organo-sedimentary structures are common in sandy and silty calcareous soils and sediments (Becze-Deák et al., 1997) and can be highly abundant in loess (Gocke et al., 2011) and desert sands (Sun et al., 2020). In addition to terrestrial settings, rhizoliths were also observed in former lacustrine environments (e.g. Sun et al., 2019a) and marine settings (Jones and Ng, 1988).

Rhizoliths have been used as proxies for paleoenvironmental reconstructions over different geological time scales based mainly on macro- and micromorphological studies (Becze-Deák et al., 1997; Barta, 2011) or stable carbon and oxygen isotope analyses (e.g. Kuleshov and Gavrilov, 2001). The large number of applications of these objects include understanding of past hydrological conditions (Li et al., 2015a) and vegetation composition (e.g. Koeniger et al., 2014) or pedogenesis (Driese and Mora, 1993).

Rhizoliths in loess–paleosol sequences are considered as important Quaternary paleoenvironmental archives (Becze-Deák et al., 1997). Several tools have been applied for paleoenvironmental reconstructions in such sequences, including stable isotopes ($\delta^{13}C$ and $\delta^{18}O$) of carbonates, pollen and bulk organic matter (OM) and specific compounds including lipid biomarkers (Pustovoytov and Terhorst, 2004; Frechen et al., 2007; Antoine et al., 2009; Zech et al., 2012). The underlying assumption of such studies is that the organic/inorganic signals present in sediments and paleosols were formed synsedimentarily and synpedogenically, respectively. Nevertheless, deep-rooting plants have the ability to penetrate sediments to a depth of several meters (Canadell et al., 1996). This was notably observed in several loess-(paleo)soil and sand-(paleo)soil sequences in Central and Southeast Europe (e.g. Gocke et al., 2014a), with high abundances of recent and fossilized roots (rhizoliths) as well as

root-derived biopores down to several meters depth below the recent soil or associated paleosol. The post-sedimentary incorporation of root-derived OM can lead to a large overprint of the initial signal in loess sediments, as shown for example for lipid biomarkers (e.g. *n*-alkanes, fatty acids, GDGTs; Huguet et al., 2013; Gocke et al., 2014b). The presence of carbonate rhizoliths in loess settings can therefore bias paleoenvironmental reconstructions. Corresponding data have to be interpreted with caution, as only limited knowledge about their formation mechanisms is available (e.g. Klappa, 1980; Gocke et al., 2011, 2014a, b; Li et al., 2015b; Sun et al., 2019a; Brazier et al., 2020).

It is generally assumed that root fossilization is controlled or induced by complex organic-inorganic interactions at the plant level (Klappa, 1980; Jaillard et al., 1991; Kautz et al., 2013; Zamanian et al., 2016; Brazier et al., 2020), but the exact processes leading to the formation of rhizoliths remain poorly constrained. Here, we report the chemical and micromorphological characterization of roots at different stages of fossilization that have been sampled at different depths (2.15 m, 3.5 m, 4 m and 8 m depth) from the extensively studied Late Pleistocene loess-paleosol sequence of Nussloch (SW Germany) (e.g. Antoine et al., 2009; Gocke et al., 2011; Zech et al., 2012; Huguet et al., 2013). The samples were chosen on the basis of their representativeness of the rhizoliths encountered along the Nussloch profile.

Scanning electron microscopy (SEM) and solid-state ^{13}C Nuclear Magnetic Resonance (NMR) techniques were used for the first time to describe and compare both the organic and mineral structures of fresh and calcified roots from the same carbonatic setting. Based on the chemical and structural information obtained from this joint organo-mineral characterization, our main goal was to disentangle the different biomineralization stages of the formation of carbonate rhizoliths of different sizes in terrestrial loess sediments.

2. Materials and methods

2.1 Study site and sampling

Recent and calcified roots were collected from a late Pleistocene loess–palaeosol sequence at the open cast mine of HeidelbergCement AG, Nussloch, SW Germany (49.19°N, 8.43°E, 217 m above sea level), as described in detail by Gocke et al. (2010, 2011, 2014a, b). The sampled profile comprises 13.1 m of loess and soil units, including the recent soil, with 3 main paleosols and 14 incipient paleosols (Gocke et al., 2014b). At the top of the profile, the recent soil is developed as 0.6 m thick Vertic Cambisol Calcaric Siltic (Gocke et al., 2013). The present vegetation, related to living roots, consists of natural broad-leaf forest and non-native robinia (*Robinia pseudoacacia*) as well as smaller shrubs and herbaceous plants and was described in detail by Gocke et al. (2013). It should be noted that present plant species were most likely not the dominant plants over the past decades or centuries due to former agricultural use. Rhizoliths at Nussloch were formed during various phases throughout the Holocene, with ages between 3 and 10 kyr (Pustovoytov and Terhorst, 2004; Frechen et al., 2007; Gocke et al., 2011) and were derived from roots of unknown trees or shrubs (likely hazel, oak, beech and alder; Gocke et al., 2013). They occur continuously from the recent soil to 8.8 m depth, with frequencies reaching up to 196 m^{-2} at 2.55 m, and are also present below 10 m underneath a major paloeosol (Lohne Soil) in lower frequencies ($\leq$ 12 m^{-2}; Gocke et al., 2014a). They can be found in various shapes and sizes (diameter between a few mm to ca. 5 cm and length from mm to several m; Gocke et al., 2011).

Three types of samples were collected in Nussloch for comparison of the organo-mineral structure of the roots: (i) present vegetation (including *Robinia pseudoacacia*); (ii) initially calcified roots and (iii) rhizoliths. Initially calcified roots correspond to living roots with a thin (< 1 mm) powdery carbonate coating on their surface. In contrast, samples termed as "rhizoliths" are fully carbonated roots with scarce or no root remains visible to the naked eye.

Preparation of the Nussloch profile for calcified root collection implied removing at least 1 m of material from the top and the side of the profile, respectively, and was followed by counting of roots, root-related biopores and rhizoliths on horizontal levels (Gocke et al., 2014b). Rhizoliths were selected for sampling in several depth intervals where no or low numbers of visible recent roots were observed in the surrounding loess, i.e. at 2.15 m, 3.5 m, 4 m and 8.8 m depth. Samples were collected and prepared as previously described (Gocke et al., 2014b). Briefly, at each depth, intact loess cores were obtained using plastic rings with an inner diameter of 20 cm and a height of 10 cm. Cores were air-dried, covered with alumina foil and kept at a cool, dry place until further preparation. After having removed the plastic ring, the uppermost 1 cm and outermost 1 cm of loess material was removed to avoid any contamination. Then, the core was cut into concentric slices from the outer parts to the interior, with the rhizolith at its center (Gocke et al., 2014b) using a ceramic knife. The rhizolith was separated from the surrounding loess by tweezers and a brush, and was then ground and homogenized (Gocke et al., 2011) or kept as intact rhizoliths for scanning electron microscopy.

Last, a loess interval at 10.4 m depth was selected for sampling the so-called “initially calcified roots”. The source vegetation of these fine roots is unknown, even though several shrub species (mainly *Buddleja sp.*) were growing at the profile wall at ca. 8-10 m depth below the recent soil. Initially calcified roots may also be present in upper layers of the Nussloch sequence, but could not be discovered during profile preparation. Therefore, the 10.4 m horizon should only be considered as a typical depth interval, where roots at an initial stage of calcification were collected. The initially calcified roots were air-dried and then divided into two pieces, one of which was ground and homogenized, while the other was kept as intact sample.

2.2 *Electron microscopy*

Root and rhizolith samples were impregnated with epoxy resin, cross-sectioned perpendicular to their longitudinal direction, polished and gold-coated for scanning electron microscopy (SEM) investigations using a Zeiss Sigma microscope operating at the Laboratoire de Geologie (ENS-Paris). Backscattered electron imaging (BEI) was carried out at 10kV and a working distance of 9.4 mm using an AsB detector. Energy Dispersive X-ray Spectrometry (EDXS) micro-analyses were performed using INCA SmartMapTM software. Elements typically encountered in secondary carbonates and surrounding loess (Ca, O, Al, Mg, Si) were traced in this study.

2.3 *Solid state ^{13}C NMR*

Roots from present vegetation and those with a thin carbonate crust were analyzed by ^{13}C NMR without any pre-treatment. In contrast, rhizoliths were treated with 3M HCl to remove carbonates which would interfere with the organic carbon signal during analysis, rinsed with ultrapure water and then frozen at -20 °C before being freeze-dried (Huguet et al., 2013). Samples were crushed in a ball mill before analysis.

Solid state ^{13}C cross polarization magic angle spinning nuclear magnetic resonance (CP MA NMR) was performed on a Bruker Avance 500 at 125 MHz for ^{13}C using 4 mm diameter zircon rotors. Cross polarization allows the magnetization transfer from ^{1}H to ^{13}C, leading to an increase in the signal/noise ratio. Magic angle spinning at 14 kHz was used to reduce chemical shift anisotropy and to average dipolar interactions, hence decreasing the linewidths. The contact time between ^{13}C and ^{1}H in the CP MAS sequence was set to 1 ms and the repetition time to 1 s. The NMR spectra were decomposed and integrated using Dmfit software – version 20150521 (Massiot et al., 2002). The subpeaks resulting from the decomposition were further grouped within 6 main regions based on existing literature (e.g. Kögel-Knabner, 2002; Lemma

et al., 2007; Mathers et al., 2007): alkyl C = 0-45 ppm (includes aliphatic and α-amino C); O/N-alkyl C = 45-90 ppm (includes methoxyl C and C in amino groups); 90-110 pm = di-O-alkyl C (includes anomeric C in carbohydrates); 110-140 ppm = aromatic and unsaturated C; 140-160 ppm = phenolic C; 160-220 ppm = carbonyl C (includes carboxylic C, amides, ketones/aldehydes). More details regarding ^{13}C NMR and its application to soil organic matter characterization can be found elsewhere (e.g. Knicker and Nanny, 1997; Kögel-Knabner, 2002; Chukov et al., 2018).

3. Results and discussion

3.1. Microscopic characterization of rhizoliths

Rhizoliths of largely variable sizes (a few cm to m long) and diameters (a few mm to cm) were observed within the Nussloch loess-paleosol sequence, as shown for example at a depth of 3.5 m (Fig. 1a). It was previously reported that rhizoliths with diameters ≥ 10 mm were predominant between 2 m and 6 m depth and rhizoliths with diameters < 10 mm were mainly observed below 6 m (Gocke et al., 2014a). Within some of the rhizoliths, the central part of the rhizolith is hollow (Fig. 1b), indicating the absence of carbonates filling the void. Even though some authors tried to classify root-related structures (Klappa, 1980) or more generally secondary carbonate accumulations (Barta, 2011) in terrestrial settings based on their external shapes, it remains difficult to classify the diversity of calcified root structures encountered in Nussloch. The general term "rhizolith" will be used here in a broad sense to refer to root traces, i.e., organo-mineral structures formed through fossilization of former roots.

Typical rhizoliths from Nussloch with diameters of 10-20 mm were analyzed for their internal structure. Independent of the depth, Scanning Electron Microscopy (SEM) revealed the presence of numerous small, fine roots encrusted by secondary carbonates within each rhizolith (e.g. Fig. 1c, f; Supp. Fig. 1). Gocke et al. (2014a) previously performed X-ray

214 microtomography scanning of one rhizolith collected at 3.5 m depth in Nussloch and observed
215 that the corresponding rhizolith contained three distinct, partially connected pores. These small
216 carbonate accumulations (diameter of <1mm) were referred to as microrhizoliths based on
217 morphological comparison with larger rhizoliths (diameter mostly 3-20 mm, up to 100 mm;
218 Gocke et al., 2014a). The present SEM results further show for the first time that, independent
219 of the depth, each rhizolith that was previously assumed to be one large individual calcified
220 root, rather consists of an assemblage of numerous "microrhizoliths", which are only visible at
221 the microscopic scale.

222 Most of these microrhizoliths roughly displayed a round shape and a central void (Fig. 1f,
223 g), indicative of the growth of the fine roots mainly in vertical direction, consistently with
224 previous observations (Gocke et al., 2011). A zoom on individual microrhizoliths reveals a
225 mosaic structure consisting of partially irregularly spread, almost concentrically arranged pores
226 and cells (Fig. 2b, c), which shows large similarities to the internal structure of recent roots
227 (Kutschera and Lichtenegger, 2002). Based on EDXS analysis, the mineral components of the
228 rhizoliths are mainly Ca-rich and Mg-poor carbonates (Fig. 3a).

229 In order to better constrain the different biomineralization processes leading to the formation
230 of the rhizoliths, the micro-elemental and -structural characteristics of microrhizoliths were
231 compared with those of (i) fresh fine roots from present vegetation at the site (*Robina*
232 *pseudoacacia* tree) and (ii) roots with a thin carbonate crust. These three types of samples
233 represent, in a simplified way, the different stages of the calcification process (Fig. 2).

234 Fresh, non-encrusted roots (Fig. 2h, i) show concentric layers of cells, with (i) a central part
235 (medulla) consisting of vascular tissues and (ii) an outer layer of cortical cells, which represents
236 the common buildup of living roots (Urry et al., 2016). The central part (Fig. 2i) is characterized
237 by secondary tissues with thick cell walls. Most of the structural characteristics of the fresh tree
238 root are still present in the initially calcified root (Fig. 2e, f). Nevertheless, some differences

239 are observed between these two types of roots. The root with a thin carbonate crust (Fig. 2d-f)
240 is characterized by (i) a thinner layer of cortical cells and (ii) larger diameter central cells in
241 comparison with the fresh fine root. Such differences could reflect the younger age of the
242 initially carbonated root compared to the fresh one or might be species-specific. Root growth
243 and development was indeed observed to result in the formation of thicker cell walls in the
244 central part, improving the mechanical strength, flexibility and storage capacity of the roots
245 (Raven et al., 2000; Kraus and Bascunsuelo, 2009). It can also not be excluded that a part of
246 the structural variations between the fresh and initially calcified roots are due to their different
247 origins (tree vs. unknown shrubs, respectively), as every plant species can display slightly
248 distinctive root morphological features (e.g. Basconsuelo et al., 2011).
249 Initially calcified roots can also be distinguished from the fresh roots by the presence of
250 calcium carbonate in some of the cortex cells (Fig. 2e, f), showing that the calcification process
251 seems to initially occur within the cortical cells and not only as a coating at the surface of the
252 root. A preliminary stage is very likely the precipitation of calcium carbonate at the surface of
253 the roots, as a thin surficial carbonatic crust was observed after sampling of the initially calcified
254 roots in Nussloch (Fig. 2d), in agreement with previous observations (Huguet et al., 2013). An
255 immediate effervescence was noted when a few drops of 3M HCl were added at the surface of
256 the crust, confirming the carbonatic nature of the latter. By combining these bulk and
257 microscopic observations, we may assume that the calcification process of the small roots is
258 initiated outside the epidermis and thereafter or simultaneously within the cortex cells.
259 A part of the initial cell and pore structure observed in the fresh root (Fig. 2h, i) was also
260 observed in microrhizoliths (Fig. 1d, e, g and Fig. 2c). Especially cortex cells filled by
261 carbonates are still visible in these microstructures (Figs. 1g and 2b), which is in agreement
262 with previous observations (Klappa, 1980; Jaillard et al., 1991; Owen et al., 2008; Cramer and
263 Hawkins, 2009). Nevertheless, in Nussloch, some of the microrhizoliths were entirely filled by

carbonates (e.g. the one highlighted in red in Fig. 1c). Most likely, the root cell structure is preserved both in the cortical and central parts of the root (Fig. 1d, e) through the precipitation of calcium carbonate (Fig. 3a). Within one single large rhizolith, numerous microrhizoliths with different structures and preservation stages can be encountered. It may not be excluded that all of the microrhizoliths detected at a given depth were not formed concomitantly. As we did not observe any root-like concentric structures in the large rhizoliths (Fig. 1c), we can exclude that a large root was responsible for the formation of the rhizolith. Either there were a lot of fine roots growing inside the decaying large root after its depth or numerous fine roots made use of the biopore that was surviving after the decay of a former root. In both cases, the largely abundant fine roots may be subsequently exposed to Ca-rich solutions in the loess, leading to the carbonate encrustation and fossilization of the former fine roots. In any case, there must be a decoupling of loess sedimentation and formation of large rhizoliths as the latter may have occurred at any point after the formation of the large biopore that was later filled by microrhizoliths, which explains the different ^{14}C ages of rhizoliths observed by Gocke et al. (2011) at Nussloch.

3.2. Characterization of organic matter by ^{13}C NMR

Fresh fine roots, initially calcified roots and rhizoliths collected at the Nussloch loess-paleosol profile were analyzed by ^{13}C NMR to investigate the effect of calcification on the composition of root organic matter. The ^{13}C NMR spectrum of *R. pseudoacacia* fine roots (Fig. 4a) presented in this study is similar to those spectra that were previously reported for roots of various higher plants (Helfrich et al., 2006; Lemma et al., 2007; Mathers et al., 2007). It was dominated by a signal ranging between 45 and 110 ppm due to N/O-alkyl C. This region comprised two main peaks (i) at 73 ppm, which can be derived from cellulose and suberin, and (ii) at 105 ppm indicative for anomeric C that can be related to hemicelluloses and other

289 carbohydrates (Baldock et al., 1992; Helfrich et al., 2006), with associated shoulders or less
290 intense peaks at 65, 84 and 89 ppm. This is consistent with the fact that macromolecules such
291 as cellulose, non-cellulosic carbohydrates (hemicelluloses, polyoses, pectines), cutin and
292 suberin are major components of plant tissues, especially in primary cell walls (Albersheim,
293 1976). The dominant peak in the aliphatic region (0-45 ppm) was observed at 30 ppm,
294 corresponding to methylene groups present in lipids (Preston and Ripmeester, 1982; Baldock
295 et al., 1992) and macromolecules such as suberin (Gil et al., 1997). Minor peaks between 25
296 and 35 ppm are similarly attributed to aliphatic compounds (Helfrich et al., 2006). Broad and
297 less intense peaks were also visible at 120-130 and 150 ppm in the aromatic and O-aryl regions,
298 respectively, and are related to aromatic molecules such as lignin and tannins. The contribution
299 of the latter type of biopolymers is further supported by the peak at 56 ppm, which can be
300 related to methoxyl groups (Zech et al., 1989; Parfitt and Newmann, 2000). The carbonyl C
301 region was dominated by a broad peak at 174 ppm that is classically attributed to esters,
302 carboxylic acids and amides, which can be found in lignin, hemicelluloses, lipids and proteins
303 (Wilson, 1987).

304 Only slight differences were observed between the ^{13}C NMR spectra of fresh and initially
305 calcified roots (Fig. 4a and b, respectively) in the 50-200 ppm region. In contrast to the fresh
306 roots (Fig. 4a), a decrease in the peak at 30 ppm and associated shoulders between 25 and 35
307 ppm and a slight increase in the peak at 15 ppm was noticed for the initially calcified roots (Fig.
308 4b). ^{13}C NMR spectra of three rhizoliths (2.15 m, 3.5 m and 4 m depth) collected at Nussloch
309 were also recorded. However, the ^{13}C NMR signals of the rhizoliths collected at 2.15 m and 3.5
310 m depth (e.g. Supp. Fig. 2) were not sufficiently resolved and the signal to noise ratio was too
311 low for a proper interpretation. Therefore, only the ^{13}C NMR spectrum of the rhizolith collected
312 at 4 m depth will be considered in the rest of this study. It exhibited broader signals in the

313 aliphatic, O/N-alkyl and carboxylic C regions (Fig. 4c) than those from fresh and initially
314 calcified roots (Fig. 4a, b).

315 In order to refine the comparison of the ^{13}C NMR spectra, the latter were deconvoluted and
316 then integrated, thus providing an estimation of the relative abundances of the different types
317 of C functional groups (expressed in % of the total area). Obvious changes in terms of relative
318 abundances of the different C functional groups were observed between the rhizolith on the one
319 hand and other roots on the other hand (Fig. 5). The rhizolith was characterized by a strong
320 decrease in the relative abundance of the O/N-alkyl and anomeric C, along with a strong
321 increase in the relative abundance of the alkyl C and aromatic C in comparison with the fresh
322 and initially calcified roots. Such differences were reflected in the much higher values of the
323 alkyl-C/(O-alkyl + anomeric C) ratio for the rhizolith (0.60) than observed for the fresh and
324 initially calcified roots (0.27 and 0.21, respectively). This ratio is classically used as a proxy
325 for soil OM degradation (Baldock et al., 1997), based on the fact that carbohydrates (i.e. O-
326 alkyl and anomeric C) are generally the first being affected by decomposition, with a
327 concomitant increase in the relative abundance of alkyl-C related possibly due to the
328 accumulation of molecules known as recalcitrant such as suberin and its derivatives (Mathers
329 et al., 2007; White, 2018). Therefore, ^{13}C NMR spectra of the different type of roots reveal that
330 preferential degradation of cellulose and non-cellulosic polysaccharides as well as enrichment
331 in suberin occurred during or after root calcification. The latter option is consistent with the
332 partial preservation of the cell wall structure of former roots through calcification, as observed
333 by SEM (Fig. 1d, e and Fig. 2f).

334 The carboxyl C relative abundance strongly depends on the root or litter type during the
335 decomposition of OM, with an absence of trends reported for some samples (e.g. Wang et al.,
336 2013) or an increase in the carboxyl C abundance for some others (e.g. Lemma et al., 2007).
337 Such an increase was partly attributed to the oxidative cleavage of lignin (Quideau et al., 2005)

and/or to the accumulation of microbial fatty acids (Zech et al., 1997) during OM decomposition. In Nussloch, no obvious difference in the carboxyl C abundance was observed between rhizoliths, fresh and initially calcified roots (Fig. 5). This might suggest that lignin was not subjected to major degradation during root calcification. This is consistent with the limited fungal activity observed along most of the Nussloch sedimentary profile according to phospholipid fatty acids biomarker analyses (Gocke et al., 2017), as fungi are considered to play a major role in lignin degradation (Su et al., 2018). Alternatively and/or complementarily, lignin might be preferentially preserved during calcification due to the degradation of more easily degradable substance classes such as sugars or fatty acids (Marschner et al., 2018). This is supported by the relative increase in aromatic C for rhizoliths vs. fresh and initially calcified roots (Fig. 5), which may be explained by the higher intrinsic chemical recalcitrance of this biopolymer vs. other compounds such as carbohydrates (Rasse et al., 2005).

Nevertheless, one should keep in mind that preservation of specific OM components in soils or sediments is dependent not only on their chemical nature but also on physical and environmental parameters (e.g. Derenne and Knicker, 2000). Consequently, in the case of the rhizoliths, the nature of the mineral matrix and the environmental conditions reflect the time of their formation, which is consistent with the study of Brazier et al. (2020), who observed a close relationship of Ca and Sr isotopes of rhizoliths with the recent soil at Nussloch.

In conclusion, ^{13}C NMR showed that OM is partially preserved during the formation of calcified roots in Nussloch, with a selective enrichment in recalcitrant and abundant root biopolymers such as lignin and suberin. This can be related to the good preservation of the cell wall structure observed by electron microscopy (Figs. 1-3). Altogether, ^{13}C NMR and SEM analyses suggest that the fossilization of the root by calcium carbonates was initiated during the same time interval as the formation of root organic tissues (during the lifetime of the root) and pursued shortly thereafter, preventing the loss of the root cell structure and major degradation

363 of OM. This is consistent with ^{14}C dating of one rhizolith from Nussloch collected at 1.5 m
364 depth, which revealed that both carbonatic and organic C ages were in the same order of
365 magnitude (3788±59 years BP and 3150±59 years BP, respectively), thus arguing for the
366 absence of postsegregational alteration (Gocke et al., 2011).
367
368 **3.3. Origin and formation of (micro)rhizoliths**
369 *3.3.1. Vegetation sources*
370 Grasses and herbaceous plants can be assumed to be potential sources of microrhizoliths in
371 the loess sequence of Nussloch (Gocke et al., 2014a), as some of these plants develop deep
372 roots (up to 2.6 m; Canadell et al., 1996), have more fine roots than trees (Jackson et al., 1997)
373 and can represent the dominant vegetation at some time periods. Nevertheless, when both
374 rhizoliths and microrhizoliths are abundant in sediments (e.g. between 1 and 6 m depth in
375 Nussloch; Gocke et al., 2014a), it is difficult to constrain the main vegetation source of these
376 calcified structures. In this case, microrhizoliths may originate not only from herbaceous plants
377 but also from fine roots of trees and shrubs based on lipid analyses (Gocke et al., 2010a, 2014b)
378 as these can have much deeper root systems up to several meters depth (Canadell et al., 1996).
379 The large, nearly round shaped structure of all rhizoliths (e.g. Fig. 1b) suggests that e.g. taproots
380 of trees formed these structures that could be traced over several meters depth within the profile.
381 It is less likely that other organisms than plants produce such connected structures with branches
382 similar to those in recent root systems and previously visualized by computed tomography
383 measurements (Gocke et al., 2014b).
384
385
386
387

388 *3.3.2. Proposed formation mechanism of calcified roots*

389 A formation mechanism of microrhizoliths and large rhizoliths in terrestrial loess sediments
390 can be proposed based on the results from the present study in Nussloch combined with those
391 of previous investigations. Three main steps can be envisioned:

392 1) After or during the growth of fine roots, a carbonate coating can develop on their surface
393 by precipitation of calcium carbonate, as suggested by bulk (HCl treatment) and
394 microscopic analyses of initially calcified roots (Fig. 2d, e, f). The initiation of the
395 calcification is directly related to rhizosphere processes and to the associated high
396 microbial activity (Jones, 1998). Roots increase acidity in the surrounding soil/sediment
397 by releasing CO_2 and exudates, which contains especially organic acids (Klappa, 1980).
398 Primary $CaCO_3$ from soil/sediment is dissolved and Ca^{2+} is being transferred in solution
399 towards the root. At the root surface not all calcium, magnesium, strontium and other
400 elements might be taken up by the plants as nutrients and can be precipitated as
401 secondary carbonates at the root surface (Barta, 2011). This is supported by the high CO_2
402 concentration in the vicinity of the root due to root and microbial respiration (Hinsinger
403 et al., 2003). In addition, Ca^{2+} and Sr^{2+} from topsoils can be taken up by plant roots and
404 translocated towards larger depths in loess-paleosol sequences as described by Brazier
405 et al. (2020). Simultaneously, or after precipitation of the carbonate coating on the
406 surface of the fine roots, surplus calcium can be precipitated as calcium carbonate within
407 the cortex cells when fine roots are still alive, as observed in Nussloch (Fig. 2g). Some
408 of the fine roots may be totally infilled by calcium carbonate, with precipitation around
409 phloem and even xylem cells, as seen for some of the Nussloch microrhizoliths (Fig. 3b).
410 This disproves the assumption of some authors that rhizoliths (or similar fossils like
411 rhizogenic calcretes) are formed exclusively after death and during or after decay of the
412 root (e.g. Joseph and Thrivikramaji, 2006).

2) When the precipitation of carbonates within the root continues, this may inhibit cycling of water, nutrients and organic matter within roots, which might lead to death of fine roots. During the decay of fine roots, organic matter as well as CO_2 gas from organic matter degradation leads to a pH decrease in the rhizosphere. Under such acidic conditions, dissolution and precipitation of calcium carbonate from sediment weathering would take place within or around the decaying roots, resulting in the mineralization and petrification of the root (e.g. Nascimento et al., 2019). Calcification of the fine roots during these two steps allows at least partial preservation of the cell wall structure (Figs. 1 and 2) and of the organic tissues (Figs. 4 and 5; Gocke et al., 2010; Huguet et al., 2012). As fine roots have an average longevity of approximately one year (Strand et al., 2008; Ding et al., 2019) and an apparent turnover of eight years (Fröberg, 2012), microrhizoliths are likely formed over a short period of time (~ 1 year).

3) Concomitantly or subsequently to the previous steps, calcium carbonate may also precipitate in voids between several of the fine roots. This is supported by the presence of a large number of microrhizoliths within one "large" rhizolith from Nussloch with precipitated carbonate in-between individual microrhizoliths (Fig. 1c, f; Supp. Fig. 1). The agglomeration of microrhizoliths may be seen as a hotspot for nutrient and water acquisition as well as microbial activity (Jones, 1998), and may promote the active growth of new fine roots in the cavities of former large roots or potentially in-between (micro-)rhizoliths, especially if they are incompletely fossilized and thus provide voids for new root growth, which was similarly observed, e.g., in a sandy profile of Sopron (NW Hungary; Huguet et al., 2013). Especially in deeper parts of the soil, biopores often serve as places for renewed root growth (White and Kirkegaard, 2010). After the death of the plants, large biopores formed by decaying roots may remain stable for millennia in fine-textured sediments such as loess (Kerényi, 2015). Also in the profile of Nussloch

many biopores were observed throughout the whole sequence, i.e. in depth intervals with high and low abundance of recent roots and rhizoliths, respectively (Gocke et al., 2014a). Consequently, it is likely in the Nussloch sequence that agglomeration of microrhizoliths occurs in biopores that were primarily produced by large tap-roots of shrubs and trees. Either during the decay of these large roots or at one point thereafter while still biopores were preserved, fine roots colonized the large biopore or decaying root, and subsequently formation of microrhizoliths occurred by the precipitation of calcium carbonate with only traces of Mg or Si (Fig. 3), whereas minerals like quartz, micas or feldspars derived from primary loess were only detected close to the outer rims of large rhizoliths (Gocke et al., 2011). Of course, it is possible that several generations of microrhizoliths can develop in one biopore of a diameter of several cm, while some older microrhizoliths might serve as additional source of nutrients on top of the surrounding sediment (Brazier et al., 2020). Thus, the carbonate remains might be partially destructed as indicated by the different status of microrhizoliths within one large rhizolith, with (i) almost intact microrhizoliths presenting perfectly round shaped structures, (ii) partially calcified microrhizoliths and (iii) residual microrhizolith structures with no clear internal structure anymore (Fig. 1).

The assemblage of numerous microrhizoliths in biopores left behind after decay of former larger roots led to the formation of larger rhizoliths, might have occurred during a large time span starting with the development of large roots and biopores after their decay shortly after sedimentation and formation of microrhizoliths at later stages. Thus, large rhizoliths in Nussloch are of Holocene age (3000-9000 yrs BP) and are much younger than surrounding loess deposited mainly during the last glacial-interglacial cycle (ca. 20,000 yrs BP; Gocke et al., 2011). A time lag of 2 kyrs between sediment deposition and its penetration by roots was also observed in a Siberian loess-like sediment (Zech et al., 2007). Similarly, in dune sands

(NW China), rhizoliths were of younger age than surrounding soil (Sun et al., 2019b). Even small calcified root cells can be formed much later than surrounding sediment (> 10 kyrs for a section close to Nussloch; Pustovoytov and Terhorst, 2004). Nevertheless, the time lag between the formation of rhizoliths and the surrounding sediment will be much larger for large roots compared to fine roots (several millennia vs. decades to centuries, respectively; Gocke et al., 2014a). In Nussloch, several rhizoliths and microrhizoliths of different size, morphology and thus very likely strongly differing age were observed within given stratigraphic units, where the calcified structures were abundant (e.g. at 3.5 m, Fig. 1a). This complicates the interpretation of paleoenvironmental and paleoecological data derived from (micro)rhizoliths and stresses the importance of fully understanding their formation in terrestrial sediments.

4. Conclusions

The organo-mineral structure of roots at different mineralization stages, collected along the Nussloch loess-palesol sequence, was documented using scanning electron microscopy and ^{13}C solid nuclear magnetic resonance. The application of SEM and ^{13}C NMR, in combination with previous results, allowed for the first time the establishment of a formation model for (micro)rhizoliths and consequently the assemblage of numerous microrhizoliths resulting in large rhizoliths: large rhizoliths were shown to consist of numerous microrhizoliths, formed mainly by calcium carbonates with only low amounts of Mg and Si. The precipitation of secondary carbonates was observed for initially calcified roots to occur first around the fine root, the epidermis acting as a first barrier, and then within the root, within the cortex cells and even sometimes around the phloem and within the xylem. Fossilization of large and fine roots by secondary carbonates was shown to allow a good preservation of root cell structure and selective enrichment of recalcitrant root biopolymers such as lignin and suberin, suggesting that the formation of (micro)rhizoliths may be initiated during the lifetime of the root and continues

after its death. This has to be systematically determined before using (micro)rhizoliths for paleoenvironmental or paleoecological reconstructions and interpreting the corresponding data with confidence. Lipid (e.g. *n*-alkanes, GDGTs, fatty acids) and compound-specific isotope analyses (including radiocarbon dating) could be used to better constrain this context.

References

Albersheim, P. (1976). The primary cell wall. In: Plant Biochemistry, Bonner and Varner eds. 3rd Edition, Academic Press, New York, 225-274.

Antoine, P., Rousseau, D.D., Moine, O., Kunesch, S., Hatté, C., Lang, A., Tissoux, H., Zöller, L. (2009). Rapid and cyclic aeolian deposition during the Last Glacial in European loess: a high-resolution record from Nussloch, Germany. Quaternary Science Reviews, 28, 2955–2973.

Baldock, J.M., Oades, J.M., Waters, A.G., Peng, X., Vassallo, A.M., Wilson, M.A. (1992). Aspects of the chemical structure of soil organic materials as revealed by solid-state ^{13}C NMR spectroscopy. Biogeochemistry, 16, 1-42.

Baldock, J.A., Oades, J.M., Nelson, P.N., Skene, T.M., Golchin, A., Clarke, P. (1997). Assessing the extent of decomposition of natural organic materials using solid state ^{13}C NMR spectroscopy. Australian Journal of Soil Research, 35, 1061–1083.

Barta, G. (2011). Secondary carbonates in loess-paleosoil sequences: a general review. Central European Journal of Geosciences 3, 129–146.

Basconsuelo, S., Grosso, M., Molina, M.G., Malpassi, R., , Kraus, T., Bianco, C., 2011. Comparative root anatomy of papilionoid Legumes. Flora, 206, 799-807.

Becze-Deák, J., Langohr, R., Verrecchia, E. (1997). Small scale secondary CaCO3 accumulations in selected sections of the European loess belt: morphological forms and potential for paleoenvironmental reconstruction. Geoderma, 76, 221-252.

Bindschedler, S., Cailleau, G., Verrecchia, E. (2016). Role of fungi in the biomineralization of calcite. Minerals, 6, 41.

Brazier, J.-M., Schmitt, A.D., Gangloff, S., Pelt, E., Gocke, M.I., Wiesenberg, G.L.B. (2020). Multi-isotope approach (δ44/40Ca, δ88Sr and 87Sr/86Sr) provides insights into rhizolith formation mechanisms in terrestrial sediments of Nussloch (Germany). Chemical Geology 545, 119641.

Canadell, J., Jackson, R.B., Ehleringer, J.R.,Mooney, H.A., Sala, O.E., Schulze, E.D. (1996). Maximum rooting depth of vegetation types at the global scale. Oecologia, 108, 583–595.

Chukov, S.N., Lodygin, E.D., Abakumov (2018). Application of 13C NMR spectroscopy to the study of soil organic matter: A review of publications. Eurasian Soil Science 51, 889-900.

Cramer, M.D., Hawkins, H.J (2009). A physiological mechanism for the formation of root casts. Palaeogeography, Palaeoclimatology, Palaeoecology, 274, 125–133.

Derenne, S., Knicker, H. (2000). Chemical structure and preservation processes of organic matter in soils and sediments. Organic Geochemistry, 31, 607-608.

Ding, Y., Leppälammi-Kujansuu, J., Helmisaari, H.-S. (2019). Fine root longevity and below- and aboveground litter production in a boreal Betula pendula forest. Forest Ecology and Management, 431, 17-25.

Driese, S.G., Mora, C.I. (1993). Physico–chemical environment of pedogenic carbonate formation in Devonian vertic palaeosols, central Appalachians, USA. Sedimentology, 40, 199–216.

Frechen, M., Terhorst, B., Rähle,W. (2007). The Upper Pleistocene loess/palaeosol sequence from Schatthausen in North Baden–Württemberg. Quaternary Science Journal, 56, 212–227.

Fröberg, M. (2012). Residence time of fine-root carbon using radiocarbon measurements of samples collected from a soil archive. Journal of Plant Nutrition and Soil Science, 175, 46–48.

Gil, A.M., Lopes, M., Rocha, J., Pascoal Neto, C. (1997). A ^{13}C solid state nuclear magnetic resonance spectroscopic study of cork cell wall structure: the effect of suberin removal. International Journal of Biological Macromolecules, 20, 293-305.

Gocke, M., Wiesenberg, G.L.B., Pustovoytov, K., Kuzyakov, Y. (2010). Rhizoliths in loess – evidence for post-sedimentary incorporation of root-derived organic matter in terrestrial sediments as assessed from molecular proxies. Organic Geochemistry, 41, 1198-1206.

Gocke, M., Pustovoytov, K., Kühn, P., Wiesenberg, G.L.B., Löscher, M., Kuzyakov, Y. (2011). Carbonate rhizoliths in loess and their implications for paleoenvironmental reconstruction revealed by isotopic composition: $\delta^{13}C$,^{14}C. Chemical Geology, 283, 251-260.

Gocke, M., Kuzyakov, Y., Wiesenberg, G.L.B. (2013). Differentiation of plant derived organic matter in soil, loess and rhizoliths based on *n*-alkane molecular proxies. Biogeochemistry, 112, 23-40.

Gocke, M., Gulyás, S., Hambach, U., Jovanović, M., Kovács, G., Marković, S.B., Wiesenberg, G.L.B. (2014a). Biopores and root features as new tools for improving paleoecological understanding of terrestrial sediment-paleosol sequences. Palaeogeography, Palaeoclimatology, Palaeoecology, 394, 42-58.

Gocke, M., Peth, S., Wiesenberg, G.L.B. (2014b). Lateral and depth variation of loess organic matter overprint related to rhizoliths revealed by lipid molecular proxies and X-ray tomography. Catena, 112, 72-85.

Gocke, M.I., Huguet, A., Derenne, S. Kolb, S., Dippold, M., Wiesenberg, G.L.B. (2017). Disentangling interactions between microbial communities and roots in deep subsoil. Science of the Total Environment, 575, 135-145.

Graça, J. (2015). Suberin: the biopolyester at the frontier of plants. Frontiers in Chemistry, 3, 62. https://doi.org/10.3389/fchem.2015.00062

Helfrich, M., Ludwig, B., Buurman, P., Flessa, H. (2006). Effect of land use on the composition of soil organic matter in density and aggregate fractions as revealed by solid-state 13C NMR spectroscopy. Geoderma, 136, 331-341.

Hinsinger, P., Plassard, C., Tang, C., Jaillard, B. (2003). Origins of root-mediated pH changes in the rhizosphere and their responses to environmental constraints: a review. Plant and Soil 248, 43–59.

Huguet, A., Wiesenberg, G.L.B., Gocke, M., Fosse, C., Derenne, S. (2012). Branched tetraether membrane lipids associated with rhizoliths in loess: rhizomicrobial overprinting of initial biomarker record. Organic Geochemistry, 43, 12-19.

Huguet, A., Gocke, M., Derenne, S., Fosse, C., Wiesenberg, G.L.B. (2013). Root-associated branched tetraether source microorganisms may reduce estimated paleotemperatures in subsoil. Chemical Geology, 356, 1–10.

Jackson, R.B.,Mooney, H.A., Schulze, E.D. (1997). A global budget for fine root biomass, surface area, and nutrient contents. Proceedings of the National Academy of Sciences of the United States of America, 94, 7362–7366.

Jaillard, B., Guyon, A., Maurin, A.F. (1991). Structure and composition of calcified roots, and their identification in calcareous soils. Geoderma, 50, 197-210.

Jones, D.L. (1998). Organic acids in the rhizosphere – a critical review. Plant and Soil, 205, 25–44.

Jones, B., Ng, K.-C. (1988). The structure and diagenesis of rhizoliths from Cayman Brac, British West Indies. Journal of Sedimentary Research 58, 457-467.

Joseph, S., Thrivikramaji, K.P. (2006). Rhizolithic calcrete in Teris, southern Tamil Nadu: origin and paleoenvironmental implications. Journal of the Geological Society of India 65, 158–168

Kerényi, A. (2015). Chapter 25. Loess Features on Tokaj Hill, in: Lóczy, D. (Ed.), Landscapes and Landforms of Hungary. Springer, Heidelberg, pp. 219–226.

Klappa, C.F. (1980). Rhizoliths in terrestrial carbonates: classification, recognition, genesis, and significance. Sedimentology, 27, 613-629.

Knicker, H., Nanny, M.A. (1997). Nuclear magnetic resonance spectroscopy: Basic theory and background. In: NMR spectroscopy in environmental science and technology. Nanny, M.A., Minear, R.A., Leenheer, J.A. (Eds). Oxford University Press, London, 3-15.

Koeniger, P., Barta, G., Thiel, C., Bajnóczi, B., Novothny, Á., Horváth, E., Techmer, A., Frechen, M. (2014). Stable isotope composition of bulk and secondary carbonates from the Quaternary loess–palaeosol sequence in Sütto, Hungary. Quaternary International, 319, 38-49.

Kögel-Knabner, I. (2002). The macromolecular organic composition of plant and microbial residues as inputs to soil organic matter. Soil Biology & Biochemistry, 34, 139–162.

Kraus, T., Basconsuelo, S. (2009). Secondary root growth in *Rhynchosia edulis* Griseb. (Leguminosae): origin of cambia and their products. Flora, 204, 635-643.

Kuleshov, V.N., Gavrilov, Y.O. (2001). Isotopic composition ($\delta^{13}C$, $\delta^{18}O$) of carbonate concretions from terrigenous deposits in the Northern Caucasus. Lithology and Mineral Resources, 36, 160–163.

Kutschera L., Lichtenegger E. (2002). Wurzelatlas mitteleuropäischer Waldbäume und Sträucher. Stocker Leopold Verlag, 604 pp.

Lemma, B., Nilsson, I., Kleja, D.B., Olsson, M., Knicker, H. (2007). Decomposition and substrate quality of leaf litters and fine roots from three exotic plantations and a native forest in the southwestern highlands of Ethiopia. Soil Biology and Biochemistry, 39, 2317-2328.

Li, Z., Wang, N., Li, R., Ning, K., Cheng, H., Zhao, L. (2015a). Indication of millennial-scale moisture changes by the temporal distribution of Holocene calcareous root tubes in the deserts of the Alashan Plateau, Northwest China. Palaeogeography Palaeoclimatology Palaeoecology, 440, 496–505.

Li, Z., Wang, N., Cheng, H., Ning, K., Zhao, L., Li, R. (2015b). Formation and environmental significance of late Quaternary calcareous root tubes in the deserts of the Alashan Plateau, northwest China. Quaternary International, 372, 165-174.

Massiot, D., Fayon, F., Capron, M., King, I., Le Calvé, S., Alonso, B., Durand, J.-O., Bujoli, B., Gan, Z., Hoatson, G. (2002). Modelling one- and two-dimensional solid-state NMR spectra. Magnetic Resonance in Chemistry, 40, 70–76.

Marschner B, Brodowski S, Dreves A, Gleixner, G., Gude, A., Grootes, P.M., Hamer, U., Heim, A., Jandl, G., Ji, R., Kaiser, K., Kalbitz, K., Kramer, C., Leinweber, P., Rethemeyer, J., Schäffer, A., Schmidt, M.W.I., Schwark, L., Wiesenberg, G.L.B. (2008). How relevant is recalcitrance for the stabilization of organic matter in soils? Journal of Plant Nutrition and Soil Science 171, 91-110.

Mathers, N.J., Jalota, R.K., Dalal, R.C., Boyd, S.E. (2007). ^{13}C-NMR analysis of decomposing litter and fine roots in the semi-arid Mulga Lands of southern Queensland. Soil Biology & Biochemistry, 39, 993–1006.

Nascimento, D.L., Batezelli, A., Ladeira, F.S. (2019). The paleoecological and paleoenvironmental importance of root traces: Plant distribution and topographic significance of root patterns in Upper Cretaceous paleosols. Catena 172, 789–806.

Owen, R.A., Owen, R.B., Renaut, R.W., Scott, J., Jones, B., Ashley, G.M. (2008). Mineralogy and origin of rhizoliths on the margins of saline, alkaline Lake Bogoria, Kenya Rift Valley. Sedimentary Geology, 203, 143–163.

Parfitt, R.L., Newman, R.H. (2000). ^{13}C NMR study of pine needle decomposition. Plant Soil, 219, 273–278.

Preston, C.M., Ripmeester, J.A. (1982). Application of solution and solid-state ^{13}C NMR to four organic soils, their humic acids, fulvic acids, humins and hydrolysis residues. Canadian Journal of Spectroscopy, 27, 99–105.

Pustovoytov, K., Terhorst, B. (2004). An isotopic study of a late Quaternary loess–paleosol sequence in SW Germany. Revista Mexicana de Ciencas Geologicas, 21, 88–93.

Quideau, S.A., Graham, R.C., Oh, S.W., Hendrix, P.F., Wasylishen, R.E. (2005). Leaf litter decomposition in a chaparral ecosystem, Southern California. Soil Biology & Biochemistry, 37, 1988-1998.

Raven, P.H., Evert, R.F., Eichhorn, S.E. (2000). Biologie végétale, 6th edition. De Boeck Université editions.

Strand, A.E., Pritchard, S.G., McCormack, M.L., Davis, M.A., Oren, R. (2008). Irreconcilable differences: fine root lifespans and soil carbon persistence. Science, 319, 456–458.

Su, Y., Yu, X., Sun, Y., Wang, G., Chen, H., Chen, G. (2018). Evaluation of screened lignin-degrading fungi for the biological pretreatment of corn stover. Scientific Reports 8, 5385.

Sun, Q., Xue, W., Zamanian, K., Colin, C., Duchamp-Alphonse, S., Pei, W. (2019a). Formation and paleoenvironment of rhizoliths of Shiyang River Basin, Tengeri Desert, NW China. Quaternary International, 502, 246-257.

Sun, Q., Wang, H., Zamanian, K. (2019b). Radiocarbon age discrepancies between the carbonate cement and the root relics of rhizoliths from the Badain Jaran and the Tengeri deserts, Northwest China. Catena, 180, 263-270.

Sun, Q., Zamanian, K., Huguet, A., Fa, K., Wang, H. (2020). Characterization and formation of the pristine rhizoliths around Artemisia roots in dune soils of Tengeri Desert, NW China. Catena 193, 104633.

Urry, L.A., Cain, M.L., Wasserman, S.A., Minorsky, P.V., Reece, J.B. (2016). Campbell Biology, 11th Edition, Chap. 35: Vascular plant structure, growth and development. Pearson Eds.

Wang, H., Liu, S., Wang, J., Shi, Z., Lu, L., Guo, W., Jia, H., Cai, D. (2013). Dynamics and speciation of organic carbon during decomposition of leaf litter and fine roots in four subtropical plantations of China. Forest Ecology and Management, 300, 43-52.

White, R.G., Kirkegaard, J.A. (2010). The distribution and abundance of wheat roots in a dense, structured subsoil–implications for water uptake. Plant, Cell & Environment, 33, 133–148.

White, K.E., Coale, F.J., Reeves III, J.B. (2018). Degradation changes in plant root cell wall structural molecules during extended decomposition of important agricultural crop and forage species. Organic Geochemistry, 115, 233-245.

Wilson, M.A. (1987). NMR Techniques and Applications in Geochemistry and Soil Chemistry. Pergamon Press, Oxford. 353 pp.

Zamanian, K., Pustovoytov, K., Kuzyakov, Y. (2016). Pedogenic carbonates: Forms and formation processes. Earth-Science Reviews, 157, 1-17.

Zech, W., Haumaier, L., Kögel-Knabner, I. (1989). Changes in aromaticity and carbon distribution of soil organic matter due to pedogenesis. Science of the Total Environment, 81/82, 179–186.

Zech, M., Rass, S., Buggle, B., Löscher, M., Zöller, L. (2012). Reconstruction of the late Quaternary paleoenvironments of the Nussloch loess paleosol sequence, Germany, using *n*-alkane biomarkers. Quaternary Research, 78, 226-235.

Zech, W., Senesi, N., Guggenberger, G., Kaiser, K., Lehmann, J., Miano, T.M., Miltner, A., Schroth, G. (1997). Factors controlling humification and mineralization of soil organic matter in the tropics. Geoderma, 79, 117-161.

Zech, M., Zech, R., Glaser, B. (2007). A 240,000-year stable carbon and nitrogen isotope record from a loess-like palaeosol sequence in the Tumara Valley, Northeast Siberia. Chemical Geology, 242, 307–318.

Captions to figures

Figure 1. Rhizoliths and microrhizoliths collected at 3.5 m depth (a, b) in Nussloch (SW Germany). Note central channel of former root growth in rhizolith in picture (b). Scanning electron micrographs showing the structure of rhizoliths collected at 3.5 m (c, d, e) and 8.8 m depth (f, g) in cross section. Zones highlighted in red in panels (c) and (f) were enlarged for better visualization of the rhizolith internal structure (cf. panels (d), (e) and (g)).

Figure 2. Pictures and scanning electron micrographs comparing the internal microstructures of rhizolith collected at 3.5 m depth (a, b, c), root at an initial stage of calcification derived from 10.4 m depth (d, e, f) and fresh tree root (*Robina Pseudoacacia*) (g, h, i), all sampled in Nussloch (SW Germany). Zones highlighted in red in middle panels were zoomed for better visualization of the rhizolith structure. Arrows indicate examples of cells filled by carbonates.

Figure 3. SEM-EDXS elemental maps of (a) a rhizolith collected at 3.5 m depth and (b) an initially calcified root collected at 10.4 m depth in Nussloch (SW Germany).

Fig. 4. ^{13}C NMR spectra of (a) fresh tree root (*Robina Pseudoacacia*), (b) root at an initial stage of calcification collected at 10.4 m depth and (c) rhizolith collected at 4 m depth in Nussloch (SW Germany).

Figure 5. Relative abundance of C functional groups obtained after deconvolution of ^{13}C NMR spectra for fresh tree root (*Robina pseudoacacia*), root at an initial stage of calcification collected at 10.4 depth and rhizolith collected at 4 m depth from Nussloch.

Supp. Fig. 1. Scanning electron micrographs showing the structure of rhizolith collected at 2.15 m depth in cross section. The zone highlighted in red in panel (a) was enlarged for better visualization of the rhizolith internal structure (cf. panel (b)).

Supp. Fig. 2. ^{13}C NMR spectrum of rhizolith collected at 2.15 m depth in Nussloch (SW Germany).

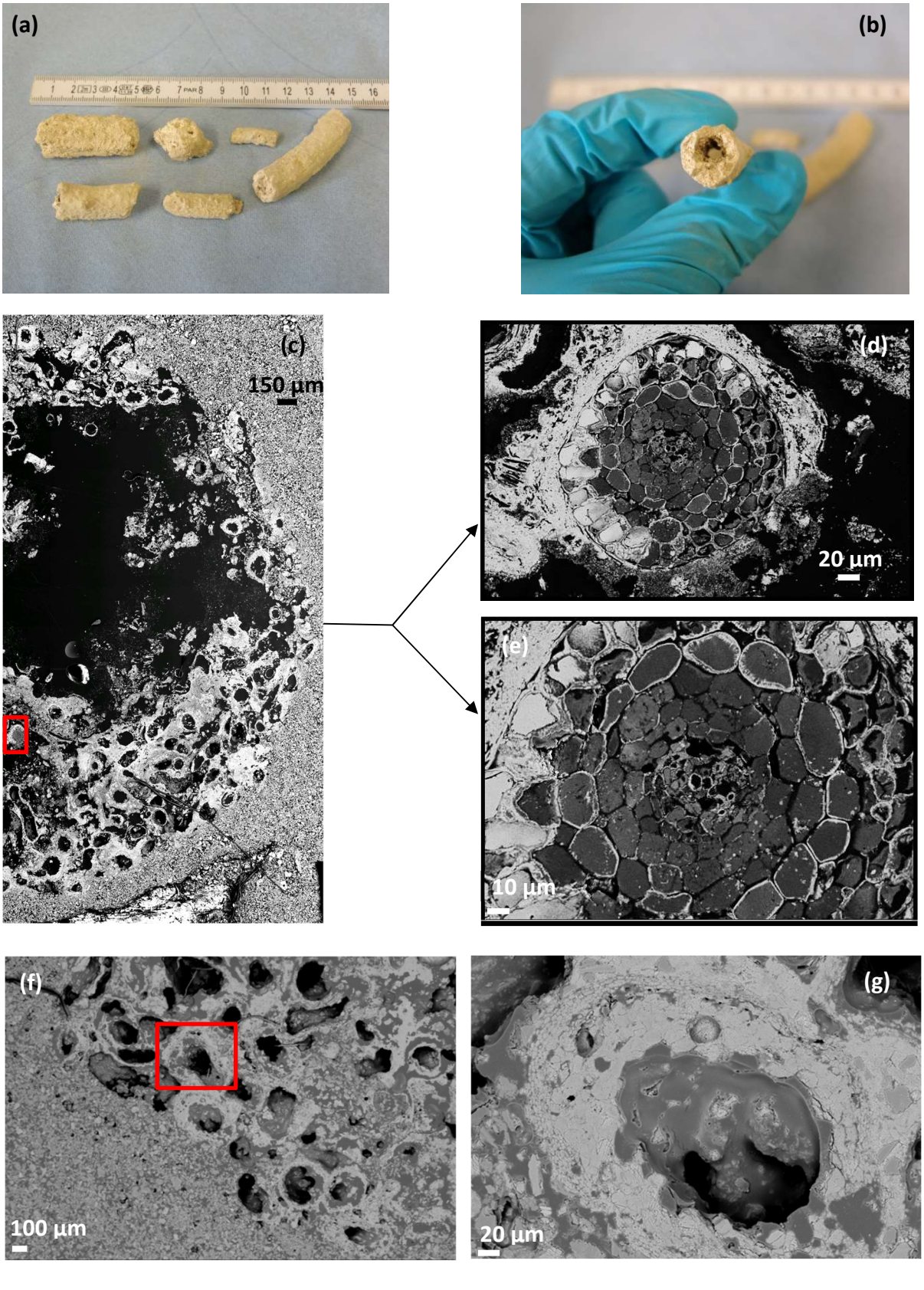
(a)
(b)
(c)
150 µm
(d)
20 µm
(e)
10 µm
(f)
100 µm
(g)
20 µm

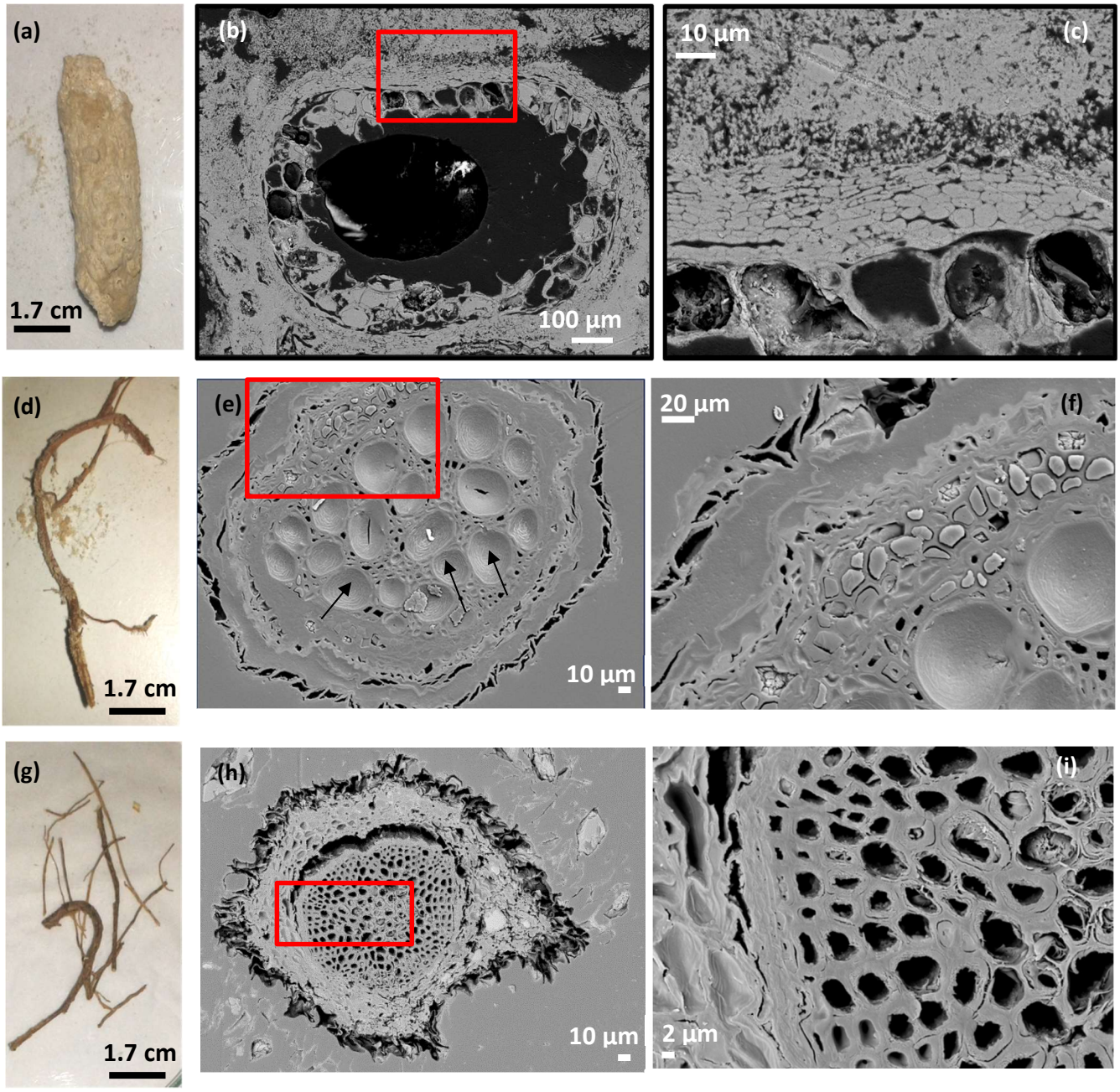
(a)
1.7 cm
(b)
100 µm
10 µm
(c)
(d)
1.7 cm
(e)
10 µm
20 µm
(f)
(g)
1.7 cm
(h)
10 µm
(i)
2 µm

(a)

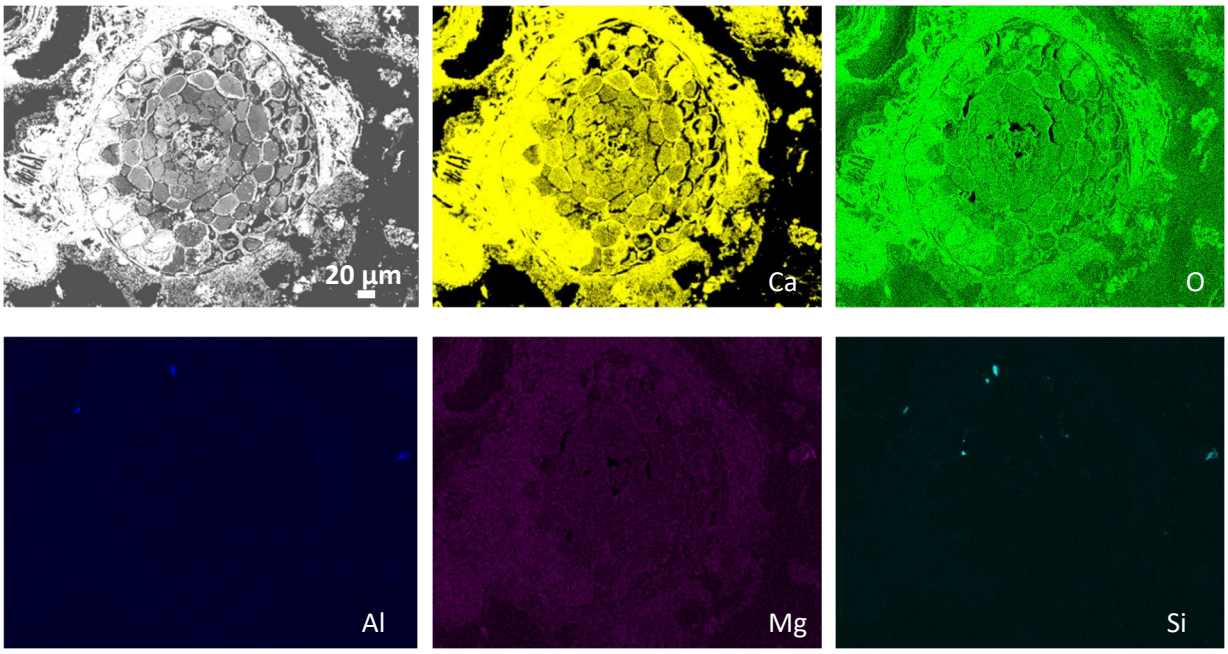

(b)

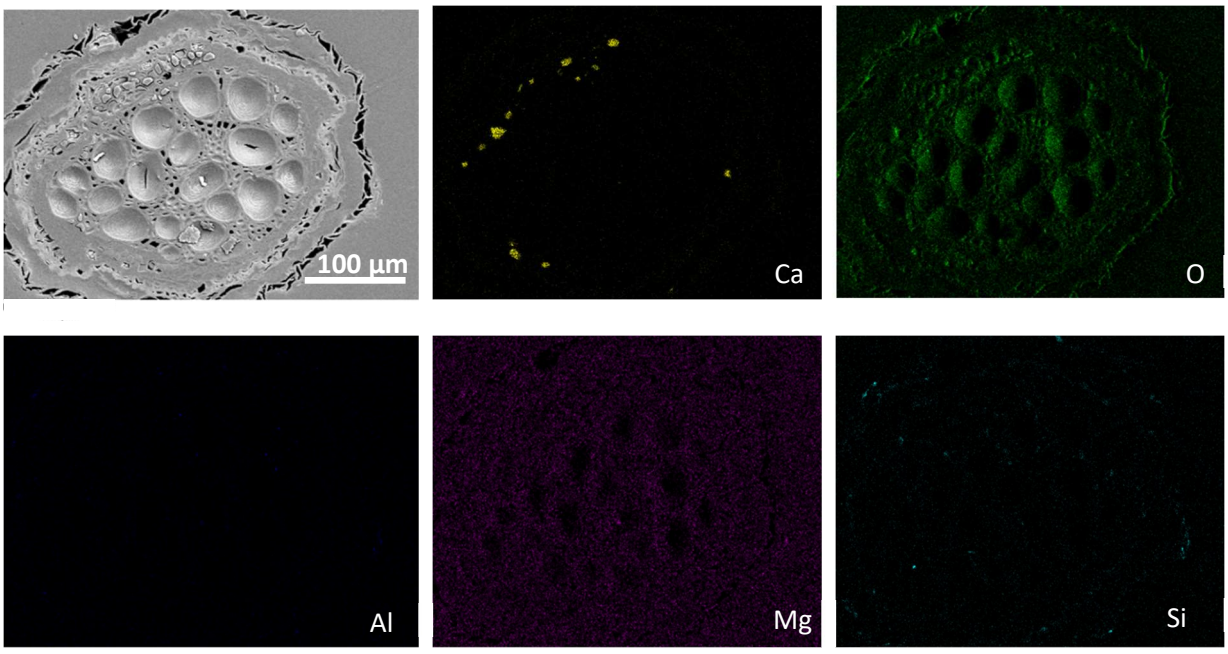

(a)

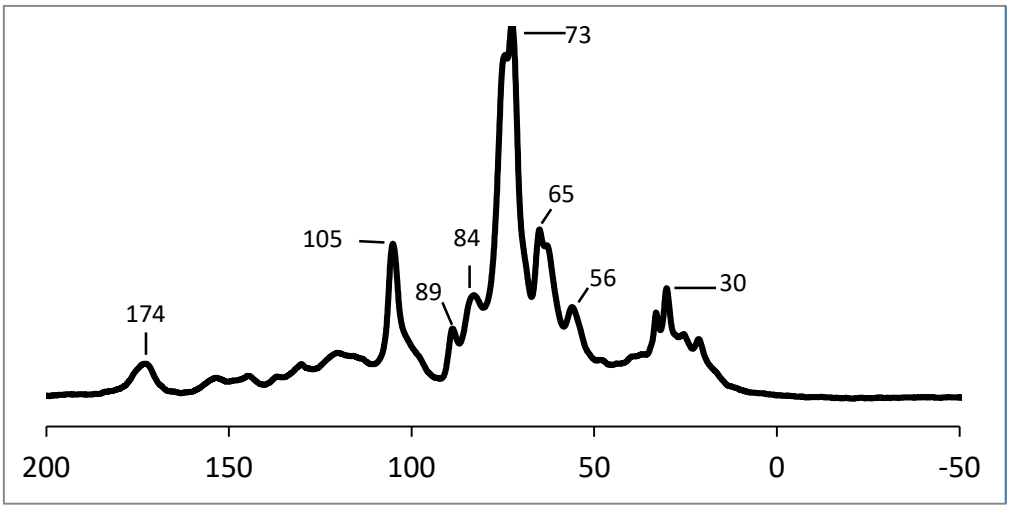
73
65
105
84
89
56
30
174
200
150
100
50
0
-50

(b)

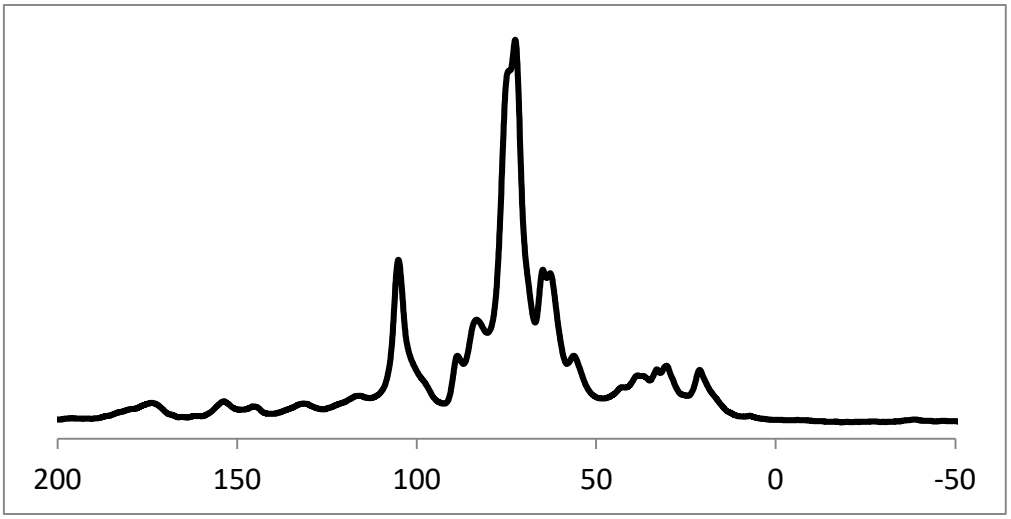
200
150
100
50
0
-50

(c)

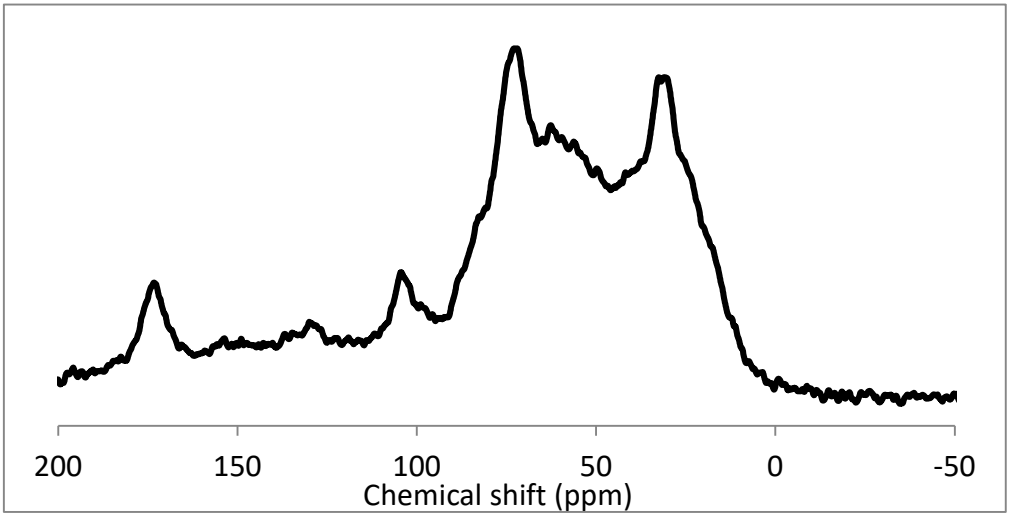
200
150
100
50
0
-50
Chemical shift (ppm)

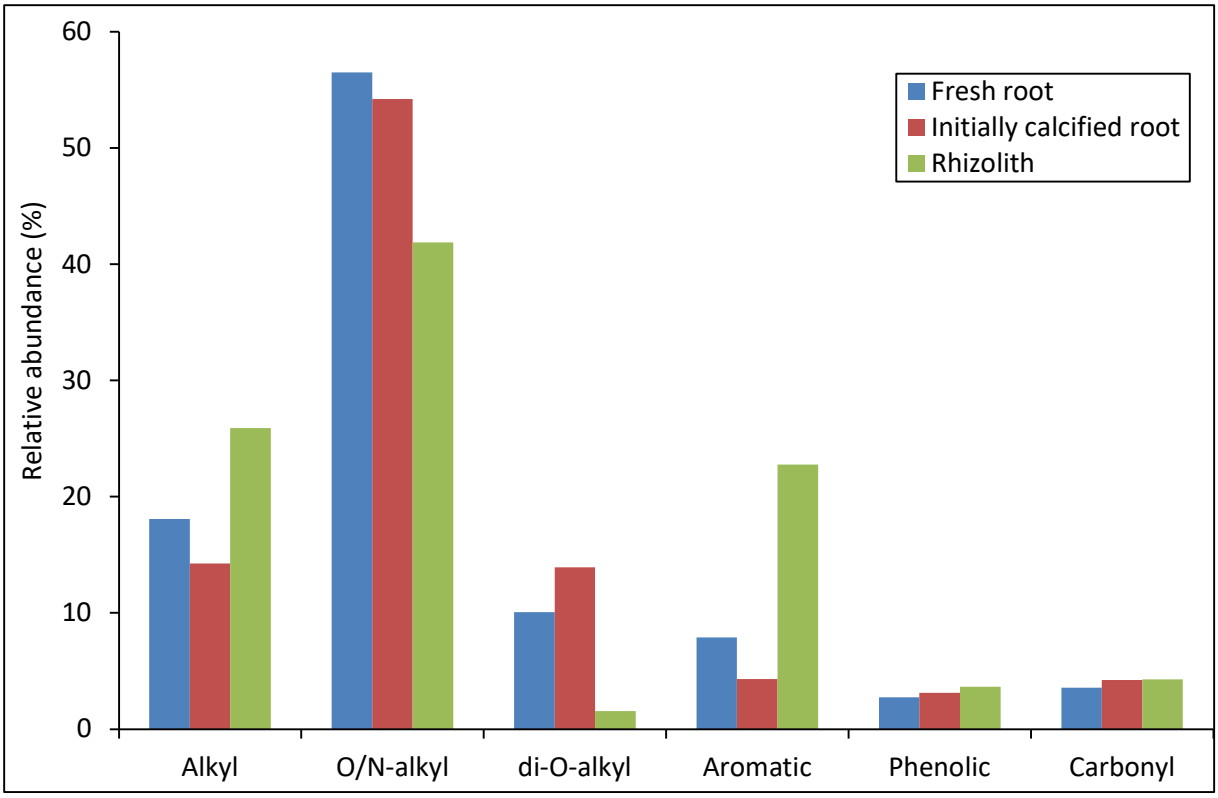
60
50
40
30
20
10
0
Relative abundance (%)
Fresh root
Initially calcified root
Rhizolith
Alkyl
O/N-alkyl
di-O-alkyl
Aromatic
Phenolic
Carbonyl

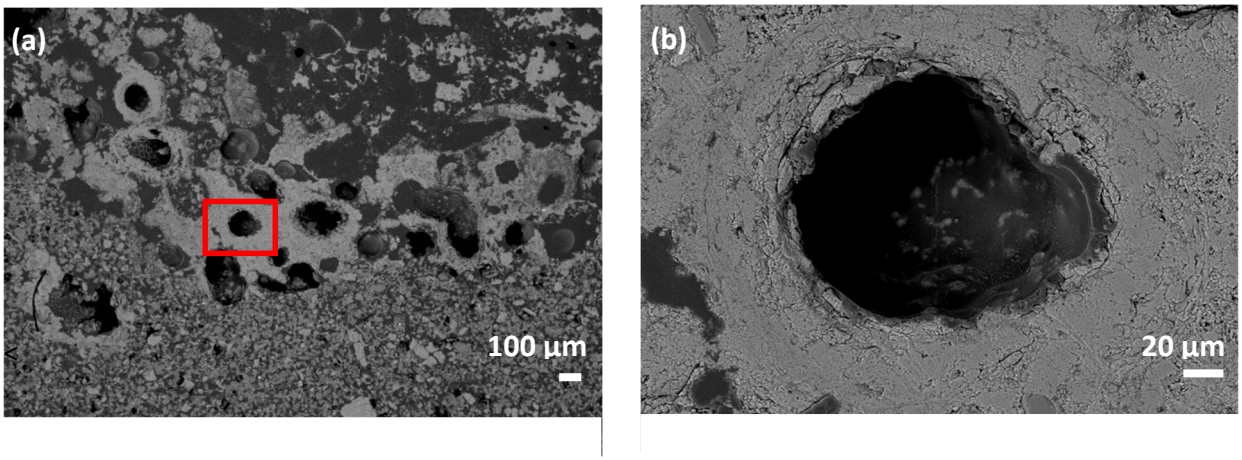

Supp. Fig. 1. Scanning electron micrographs showing the structure of rhizolith collected at 2.15 m depth in cross section. The zone highlighted in red in panel (a) was enlarged for better visualization of the rhizolith internal structure (cf. panel (b)).

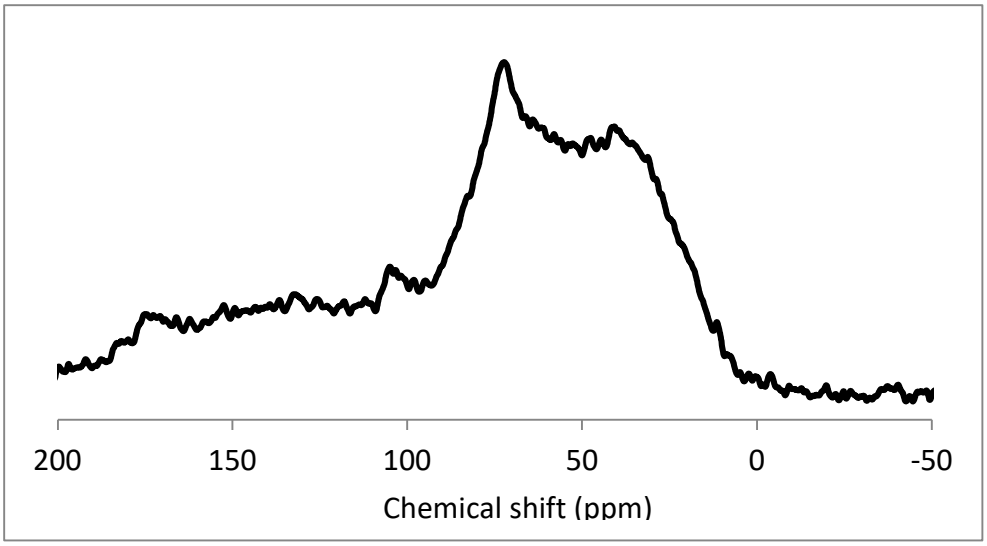

Supp. Fig. 2. ^{13}C NMR spectrum of rhizolith collected at 2.15 m depth in Nussloch (SW Germany).